Observing the behaviour of reinforced magnesium alloy with carbon-nanotube and lead under 976 m/s projectile impact

M.F. Abdullah[1], S. Abdullah[2], M.Z. Omar[2], Z. Sajuri[2], M.S. Risby[1]

[1]Department of Mechanical Engineering,
Faculty of Engineering,
Universiti Pertahanan Nasional Malaysia,
Kem Sg. Besi 57000 Kuala Lumpur, Malaysia

[2] Department of Mechanical and Materials Engineering,
Faculty of Engineering & Built Environment,
Universiti Kebangsaan Malaysia.
43600 UKM Bangi, Selangor, Malaysia

ABSTRACT

This paper presents the effects of reinforced magnesium alloy, AZ31B with carbon-nanotube (CNT) and lead (Pb), in terms of ballistic resistance. Magnesium alloys possess high energy absorption capability for impact resistance. However, its capability is limited and needs to be enhanced to resist ballistic impacts. The addition of a reinforcement material within the magnesium alloy, such as CNT or Pb, can improve impact resistance. This study is divided into two ballistic test methods, namely experiment and simulation. The samples involved are the original AZ31B and reinforced AZ31B with CNT and Pb. The projectile type used for ballistic testing was a 5.56 mm FMJ NATO at a velocity of 976 m/s and the thickness of the plate was 25 mm. The aim is to study the ability of the plate against the ballistic resistance. The ballistic experiment utilises a high speed camera, at 100,000 fps, to capture the impact occurring on the plate's surface. A Cowper-Symonds model is used for the ballistic simulation and indicates the ballistic resistance of the reinforced AZ31B with increments of CNT and Pb. The velocity of the projectile penetrating through the plate was reduced by over 45% compared to the original AZ31B alloy. Reinforcement using CNT and Pb on AZ31B improved the ballistic resistance behaviour and therefore, this material is suitable for use on ballistic panels

ISSN 1823- 5514, eISSN 2550-164X
Received for review: 2017-05-05
Accepted for publication: 2017-08-15
Published: 2018-01-31

Keywords: *Ballistic resistance, Carbon-nanotube, Lead, Cowper-Symonds model, Magnesium alloy.*

Introduction

Magnesium-based alloys are of current interest to the military industry because they are the lightest of all structural metal alloys [1]. The density of magnesium is approximately 35% lower than that of aluminium and approximately 77% lower than that of steel [2,3]. Magnesium alloy is the lightest metallic material that has a high potential for weight reduction; thereby decreasing the amount of fuel required in automobile and aerospace applications. However, compared to several conventional materials, such as steel, fewer studies have been performed on the relationship between magnesium alloys and impact loading [4]; particularly under ballistic conditions.

Magnesium has a hexagonal close-packed (HCP) structure. In HCP inorganic compounds, larger atoms (or ions) occupy positions corresponding approximately to those of equal spheres in close packing, while smaller atoms are distributed among the voids [5]. For example, a material that can fill these voids is necessary to prevent structure collapse, such as carbon nanotubes (CNTs) with a nano-material structure. CNTs have unique properties that can produce strong materials and improve the energy absorption of other materials [6–8]. The molecular nanotechnology of CNTs can fill the spaces in a structure and produce van der Waals bonds therein [9–11]. The high energy absorption efficiency of magnesium alloy confers excellent anti-penetration performance of the material [4]. However, the most efficient energy absorption is achieved by adding high-density elements, such as lead (Pb), gold, rare-earth elements, and others [7]. Magnesium alloy offers a unique combination of high tensile strength (up to 410 MPa), low density (up to 1.8 g/cm3), and superior shock absorbency of 100 times greater than aluminium alloys [8]. Magnesium also has the highest specific damping capacity of the metals used in armour applications. Thus, magnesium is an excellent choice for ballistic applications because of its enhanced energy absorption and shock mitigation. Previous studies [4–6] on magnesium alloy characterisation indicated the determined appropriate properties for ballistic applications. This alloy is suitable for application in armour plating to reduce armour weight whilst increasing the fuel consumption efficiency of armoured vehicles, and providing ballistic resistance.

Rolled homogeneous armour (RHA) is steel-based and is currently used on armour plating. Replacing RHA with magnesium alloy offers a new alternative that solves armour weight and fuel consumption problems whilst providing the same penetration resistance. It is known that AZ31B is a

material that can potentially replace RHA for armoured vehicles because of its impact behaviour [7,8]. However, the composition of AZ31B has less strength to support the impact deformation structure. A combination of CNT and Pb on magnesium alloy may exhibit a high reduction of impact resistance. Therefore, CNT and Pb could be added to AZ31B to obtain increased ballistic resistance. The objective of this study is to observe the behaviour of magnesium alloy reinforcement with CNT and Pb under ballistic impact. The results demonstrate the deformation of magnesium alloy under ballistic and stress distributions. The addition of CNT and Pb provide the magnesium alloy material with good ballistic resistance.

Methodology

Figure 1 shows the process flow for this study. The study is divided into two main sections that address ballistic simulation and experiment. The target plates tested were magnesium alloy, AZ31B and reinforced AZ31B with CNT and Pb. The percentage of CNT and Pb used as reinforcement on AZ31B were approximately 0.2 and 0.5 %, respectively. This percentage range gave good van der Waals bonding of the material and reinforced the material by filling the nano voids in the AZ31B [4,6].

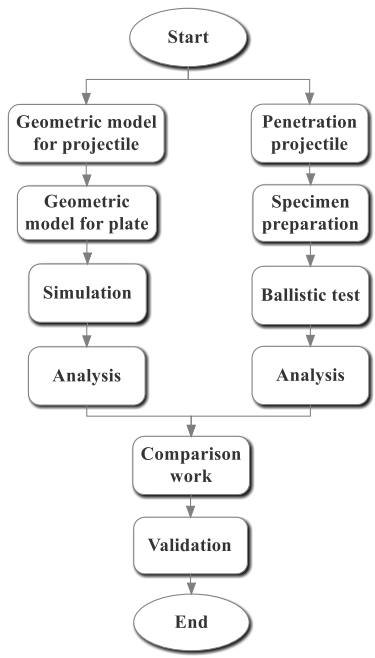

Figure 1 A simplified process flow for this research procedure

The ballistic experiments were performed using Level III, according to the NIJ standard [12]. These experiments used a sample size of 100 mm (L), 100 mm (W) and 25 mm (t) as shown in Figure 2. The ballistic test on Level III used a projectile type of 5.56 mm FMJ NATO (as shown in Figure 3). Figure 4 shows a schematic sketch and position caused by the ballistic experiments. The sample, positioned 5 metres from the gun barrel, was placed near to the velocity measuring device to determine the velocity of the projectile hitting the sample. In addition, a high-speed camera was used (at 100,000 frames per second) to view the projectile's penetration process on the sample. The velocity of the projectile was 976 m/s, which meets NIJ standard Level III.

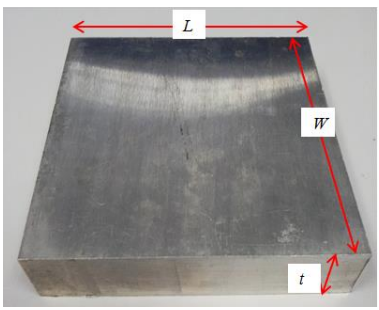

Figure 2 The sample size used for ballistic testing was L= 100 mm, W=100 mm, t=25 mm

Figure 3 The type of projectile used was 5.56 mm FMJ NATO

From the simulation, two models were used, Johnson-Cook and Cowper-Symonds. The projectile materials, which were copper and lead, used the Johnson-Cook model because many researchers completed impact simulation using the same projectile materials and established good parameters [13,14]. On the plate samples, the Cowper-Symonds model was utilised. The parameters of the Cowper-Symonds model were determined from tensile and Split Hopkinson Pressure tests. However, Tan (2015) concluded that ballistic impact simulation conducted using the Johnson-Cook and Cowper-Symonds models did not give a significant difference [14]. Table 1 shows the materials

used in the ballistic simulations for the 5.56 mm FMJ NATO and the plate. Figure 5 shows a simulated ballistic use of the projectile 5.56 mm FMJ NATO.

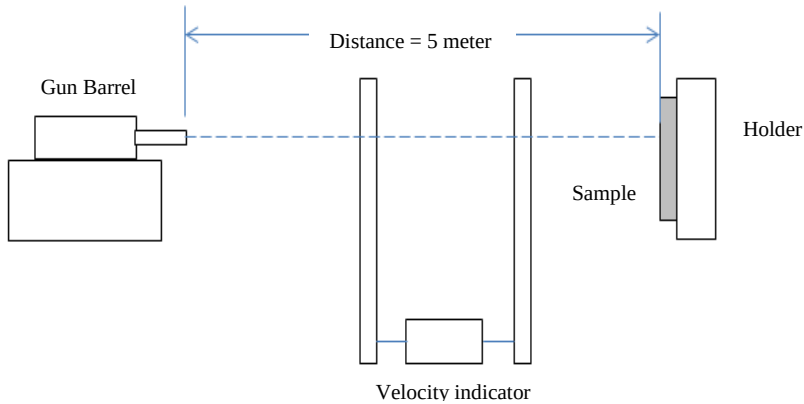

(a)

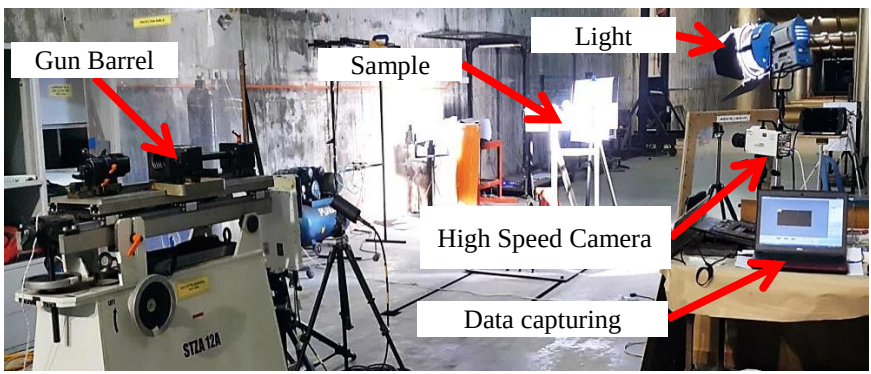

(b)

Figure 4 The experiment of ballistic (a) Schematic diagram (b) ballistic testing equipment.

The Johnson-Cook model is represented by the following eq. (1):

$$\sigma = \left(A + B\varepsilon_p^n\right)\left(1 + C\ln\dot{\varepsilon}^*\right)\left(1 - T^{*m}\right) \quad (1)$$

where σ_{eq} is the equivalent stress, ε_{eq} is the equivalent plastic strain, A, B, n, C and m are the material constants and $\dot{\varepsilon}^{*}_{eq} = \dot{\varepsilon}_{eq}/\dot{\varepsilon}_0$ is the dimensionless strain rate as a ratio of the strain rate and user-defined strain rate. T^{*m} is the homologous temperature and is given as $T^{*m} = (T - T_r)(T_m - T_r)$, where T_r and T_m represent the room temperature and the melting temperature, respectively [14]. In addition, the Cowper-Symonds model is represented by the following eq. (2):

$$\sigma_y = \sigma_0 \left[1 + \left(\frac{\dot{\varepsilon}}{C} \right)^{\frac{1}{q}} \right] \tag{2}$$

where C and q are the Cowper-Symonds coefficients, $\dot{\varepsilon}$ is the strain-rate, σ_y is the dynamic stress or strength, and σ_0 is the quasi-static stress or strength [14]. The coefficients obtained for Eqs. 1 and 2 are presented in Table 1.

Table 1 Parameter for Cook-Johnson and Cowper-Symonds model for material properties.

Materials	Johnson-Cook [13]		Cowper-Symonds	
	Copper	Lead	AZ31B	AZ31B + % CNT + % Pb
Strain Hardening, B (MPa)	303.40	413.00		
Strain hardening exponent, n	0.150	0.210		
Constant rate of strain, C	1.030	1.030	1.599	3.469
Thermal softening constant, m	0.003	0.003		
Melting temperature, T_m (K)	1358.05	596.05		
Strain rate exponent, q	-	-	7124.556	3574.729

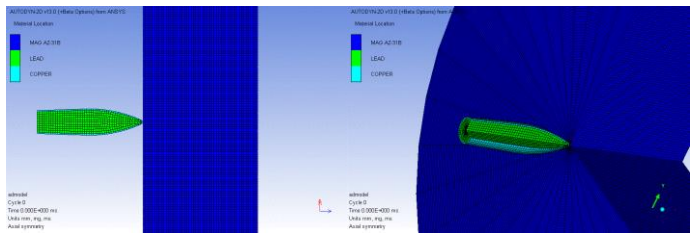

(a) (b)

Figure 5 Geometrical modelling using the projectile types 5.56 mm FMJ NATO under different shape: (a) 2-dimensional, (b) 3-dimensional

Results and Discussion

Figure 6 shows the effect of the ballistic impact on the reinforced AZ31B + CNT + Pb plates using ballistic experiment and simulation. It has been shown that the front and back plate conditions, obtained from the experiment, are similar to those of the simulation. It has been shown that the front plate has a smaller diameter than the back plate. This is because early impact projectiles gave small deformations, and the deformation of the projectile was expended through the plate's thickness.

Figure 7 shows the effect of the ballistics on the AZ31B plate from both experiment and simulation. It has been shown that the back AZ31B + CNT + Pb plate from the experiment had a formation of material deformation identical to the simulation's results. However, the back AZ31B plate indicated fragments that were not seen in the simulation. This condition occurred because the AZ31B + CNT + Pb plate had a mixed structure that could provide additional ductile properties to the material. Therefore, even the back area of the plate still experienced high stress, and the materials still had bonds with each other. Compared to the magnesium alloy plate, AZ31B on the backside was slightly plugged off, which resulted from the high stress and less ductility behaviour than the AZ31B + CNT + Pb. As this phenomenon occurred on the back of the plate, it had the tendency to cause injury to anyone nearby, with debris thrown at quite a high velocity. Therefore, the ductility of a material is also taken into account in the selection of ballistic protection materials. These behaviours show that the AZ31B alloy material, with a mixture of CNT and Pb, had better ballistic impact resistance.

Table 2 shows the simulation and experimental data for AZ31B and AZ31B + CNT + Pb from performing ballistic impact tests using projectile type 5.56 mm FMJ NATO. The results show that the penetration effect on AZ31B was greater than on the AZ31B + CNT + Pb. Figure 8 shows the correlation graph between the front diameter and back diameter of the plates resulting from experiments and simulations. Correlation between experiment

and simulation is important to determine the accuracy of the simulation by taking the experimental data as a reference. It was found that the front and back diameters of the AZ31B + CNT + Pb and AZ31B plates fitted well with R^2 of 0.9989. A slight difference occurred for the back of the AZ31B plate, because the stress on the back of the plate is more than the yield stress of the material, and failure occurs in the vicinity of the back end. This causes the penetration diameter to be unchanged compared to the simulation result. This phenomenon is clearly visible on the back of the AZ31B plate.

Table 2 Diameter penetration of AZ31B + CNT + Pb and AZ31B for ballistic using 5.56 mm NATO FMJ projectile.

Material	Front diameter (mm)		Back diameter (mm)	
	Simulation	Experiments	Simulation	Experiments
AZ31B	6.50	7.00	15.00	17.00
AZ31B+CNT+Pb	6.40	6.80	10.00	11.40

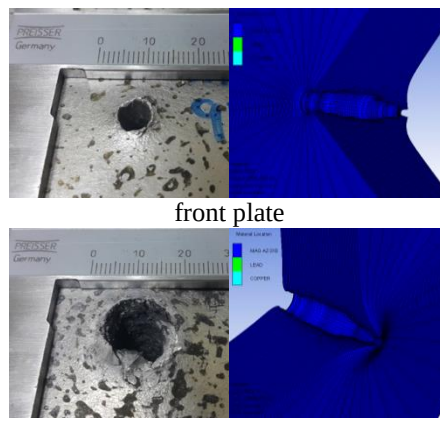

Figure 6 Deformation effect of ballistic impact on AZ31B + CNT + Pb plate for; (a) experiments (b) simulation.

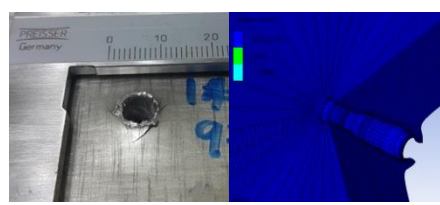

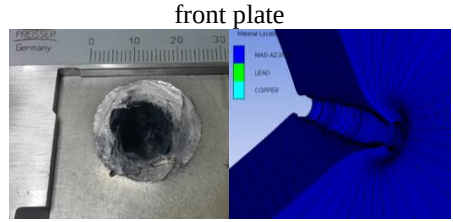

(a) (b)

Figure 7 Deformation effect of ballistic on AZ31B plate for (a) experiments (b) simulation

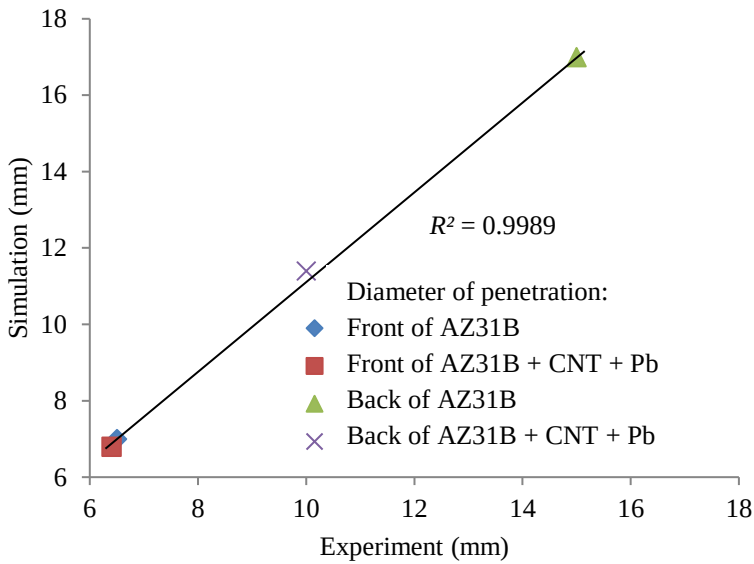

Figure 8 Correlation diameter penetration between simulation and experiment on front and back plate for AZ31B + CNT + Pb and AZ31B.

Figure 9 shows the movement during the test projectiles penetrating the AZ31B + CNT + Pb and AZ31B plates captured by high-speed camera. These images were taken at an oblique angle of 30 degrees to protect the camera from any plat shrapnel or projectile reflection (as shown in Figure 4 (b). During the experiment, a small explosion took place when the projectile hit the plate. This phenomenon, known as early burning, also affected the experiment's results, but was not observed in the simulation.

Figure 10 shows the reduction of velocity when the projectile penetrated the AZ31B + CNT + Pb and AZ31B plates. The minimum penetration velocity of the projectile through the AZ31B + CNT + Pb plate was 182.48 m/s, while the minimum penetration velocity of the projectile through the AZ31B plate was 354.67 m/s. The percentage of reduction in projectile velocity through the AZ31B + CNT + Pb material was 48.55% compared to the original material. This was because the CNT affected the material bonding to reduce the deformation on impact, and Pb affected the ductility to absorb the velocity of the projectile.

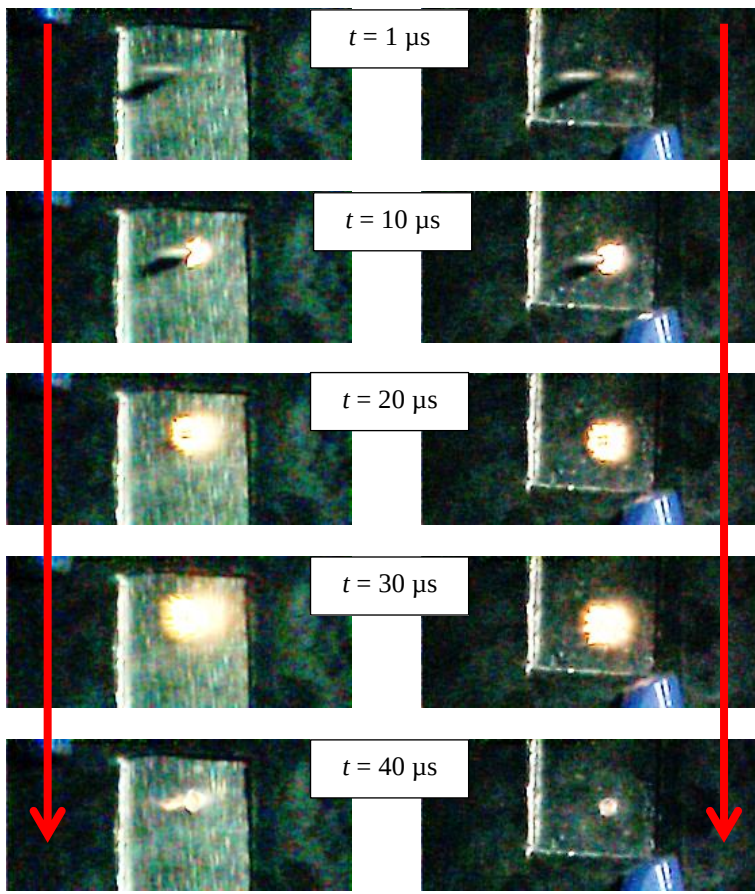

Figure 9 Projectile penetration on AZ31B + CNT + Pb and AZ31B plates, captured by the high-speed camera.

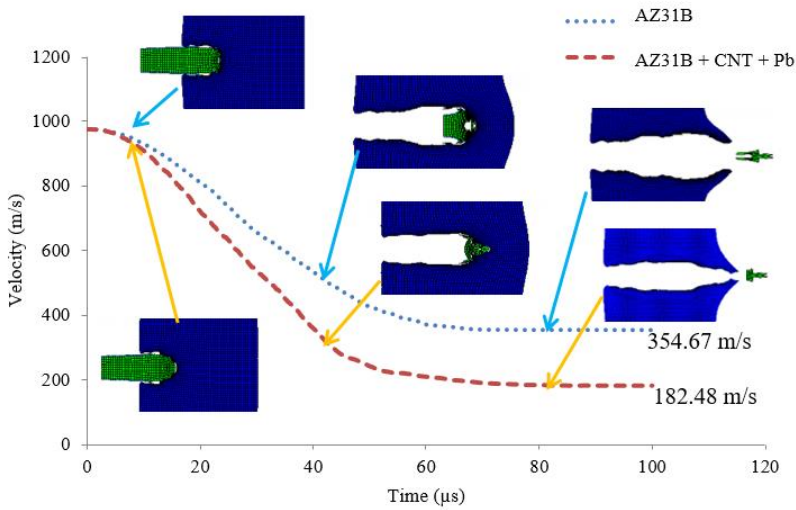

Figure 10 Comparison of projectile penetration through AZ31B + CNT + Pb and AZ31B plate.

The ballistic experiment, for plates consisting of magnesium alloy, AZ31B and magnesium alloy AZ31B mixed with CNT and Pb, showed that reinforced magnesium alloy had higher ballistic impact resistance than the original magnesium alloy. This proves that the reinforcement materials of CNT and Pb in AZ31B magnesium alloy are suitable to improve the ballistic impact resistance of the original alloy.

Conclusion

The effect of CNT and Pb, added to the behaviour of AZ31B alloy, on ballistic impact resistance was investigated. The addition of CNT and Pb in AZ31B improved ballistic resistance using the projectile type 5.56 mm FMJ NATO, and reduced the speed outlet at the plate by approaching 50%. This situation is based on the valuation simulation. However, for correlation between simulation and experiment, not much difference was observed, where the R^2 obtained was above 0.9500. Our results show that magnesium

alloy is a suitable material for ballistics and military applications. Furthermore, the addition of an element into the original alloy composition enhances the behaviour of the material in terms of ballistic impact.

Acknowledgments

The authors would like to express their gratitude to Ministry of Higher Education Malaysia via Universiti Kebangsaan Malaysia and Universiti Pertahanan National Malaysia (Research funding: LRGS/2013/UPNM-UKM/DS/04) for supporting this research.

References

[1] M.A. Honsel GmbH & Co KG Meschede. Weight and cost saving with magnesium die castings. Proc.5th Int. Conf. Magnesium Alloys and Their Applications; 397-401 (2000).

[2] T.L. Jones, R.D. DeLorme, M.S. Burkins, Ballistic Evaluation of Magnesium Alloy AZ31B. Army Research Laboratory ARL-TR-4077; 1-14 (2007).

[3] H. Watari, K. Davey, M.T. Rasgado, S. Izawa, Semi-solid manufacturing process of magnesium alloy by twin-roll casting. J. Material Processing Technology; 155-156: 1662-1667 (2004).

[4] F. Yatu, Q. Wang, J. Ning, J. Chen, W. Ji, Experimental measure of parameters: The Johnson-Cook material model of extruded Mg-Gd-Y series alloy. ASME J. Applied Mechanics; 77:051902-1-5 (2010).

[5] P.K. Jena, K. S. Kumar, V. R. Krishna, A.K. Singh and T. B. Bhat. Studies on the role of microstructure on performance of a high strength armour steel. Engineering Failure Analysis 15; 1088–1096 (2008).

[6] Q. Li, C.A. Rottmair, R.F. Singer. CNT Reinforced Light Metal Composites Produced by Melt Stirring and by High Pressure Die Casting. Composites Science and Technology; 1-17 (2012).

[7] M. Rahman, M. Hosur, S. Zainuddin, U. Vaidya, A. Tauhid, A.Kumar, J. Trovillion, S. Jeelani. Effects of amino-functionalized MWCNTs on ballistic impact performance of E-glass/epoxy composites using a spherical projectile. International Journal of Impact Engineering 57; 108-118 (2013).

[8] E.M. Soliman, M.P. Sheyka, M. R. Taha. Low-velocity impact of thin woven carbon fabric composites incorporating multi-walled carbon nanotubes. International Journal of Impact Engineering 47; 39-47 (2012).

[9] A.F Avila, M.I. Soares, A.S. Neto, A study on nanostructured laminated plates behaviour under low-velocity impact loadings. Int J Impact Eng;34: 28-41(2007)
[10] Patent N0.2 US 7,921,899 B2. Method for marking magnesium-based carbon nanotube composite material. United States Patent 2011. Pp 1-6.
[11] V. Tan, T. Ching. Computational simulation of fabric armour subjected to ballistic impacts. Int J Impact Eng;32:1737-51 (2006).
[12] NIJ Standard-0101.06. Ballistic Resistance of Body Armor; 1-89 (2008).
[13] F. Feng, S. Huang, Z. Meng, J. Hu, Y. Lei, M. Zhou & Z. Yang. A constitutive and fracture model for AZ31B magnesium alloy in the tensile state. Materials Science and Engineering: A 594: 334-343 (2014).
[14] J. Q. Tan, M. Zhan, S. Liu, T. Huang, J. Guo & H. Yang. A modified Johnson–Cook model for tensile flow behaviors of 7050-T7451 aluminum alloy at high strain rates. *Materials Science and Engineering: A* 631: 214-219 (2015).
[15] T. L. Jones, R. D. DeLorme, M. S. Burkins & W. A. Gooch. Ballistic performance of magnesium alloy AZ31B. 23rd International Symposium on Ballistics; 989 – 995 (2007).
[16] H. Asgari, A. G. Odeshi, J. A. Szpunar, L. J. Zeng & E. Olsson. Grain size dependence of dynamic mechanical behavior of AZ31B magnesium alloy sheet under compressive shock loading. Materials Characterization 106: 359-367 (2015).